3746 *J. Am. Chem. Soc.* **1993,** *115,* 3746-3751

Reaction Pathways for Gas-Phase Hydrolysis of Formyl Compounds HXCO (X = H, F, and Cl)

Joseph S. Francisco[*,1a] **and Ian H. Williams**[1b]

Contribution from the Department of Chemistry, Wayne State University,
Detroit, Michigan 48202, and the School of Chemistry, University of Bath,
Bath BA2 7AY, United Kingdom

Received December 5, 1991

Abstract: Formation and decomposition of the adduct species $CHX(OH)_2$, where X = H, F, and Cl, have been studied by means of ab initio molecular orbital theory. Equilibrium geometries and transition structures have been fully optimized with 6-31G* and 6-311G** basis sets at the Hartree–Fock and second-order Møller–Plesset perturbation levels of theory. Heats of reaction and barrier heights have been computed with Møller–Plesset theory up to full fourth order using the 6-311++G** basis. Addition of H_2O to HXCO yields $CHX(OH)_2$ which then decomposes preferentially by 1,2-elimination of HX to give formic acid as a product. Other higher energy paths, including 1,2-elimination of H_2 and the involvement of carbene species, are of negligible significance.

Introduction

Tropospheric degradation of proposed CFC alternatives such as CF_3CHXY (where X, Y = H, F, or Cl) leads to the formation of carbonyl compounds HXCO whose atmospheric fates are governed largely by their reactivities toward hydrolysis.[2,3] Previous theoretical studies have focused upon the addition of water to formaldehyde[4,5] or to formyl fluoride[6] yielding the hydrate [$CHX(OH)_2$, reaction 1 in Scheme I]. In this paper the energies of reactions 1–4 are examined in detail for X = H, F, and Cl by means of ab initio MO theory with electron correlation. The barriers for reactions 5 and 6 have been calculated and shown to be consistent with experimental results.[7] Decomposition 7 of the products HCO_2H and XCO_2H of reactions **2** and **3** has also been examined in recent theoretical studies.[8-10]

Scheme I

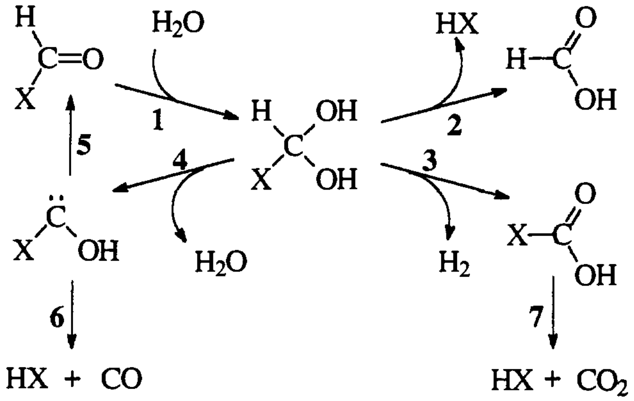

Methods

All calculations were performed with the GAUSSIAN 88 or GAUSSIAN 90 programs.[11] Geometry optimizations were carried out for all structures by using Schlegel's method with convergence criteria of better than 0.001 Å for bond lengths and 0.1° for angles.[12] All optimizations were performed with split-valence and polarized basis sets, i.e., 6-31G**[13] and 6-311G**.[14] Equilibrium and transition-state geometries were fully optimized at the Hartree–Fock and second-order Møller–Plesset (MP2) levels with all orbitals active. Single-point energy calculations were performed for MP2-optimized geometries at the MP4 level including all single, double, triple, and quadruple excitations, using the frozen-core approximation.[15,16] All harmonic vibrational frequencies were obtained at the HF/6-31G* level of theory.[17,18]

Results and Discussion

The optimized geometries for equilibrium structures and transition structures are presented in Tables I and II, with the corresponding total energies in Table III. The MP2/6-31G* and MP2/6-311G** geometries are generally very similar, the largest differences being for the partial bonds in the transition structures. Vibrational frequencies are collected in Table IV, and relative energies and barrier heights are listed in Table V.

---

(1) (a) Wayne State University. (b) University of Bath.

(2) Atkinson, R. In *Scientific Assessment of Stratospheric Ozone,* Vol. II; AFEAS Report: World Meterological Organization, Report No. 20, 1989.

(3) Cox, R. A.; Lesclaux, R. In *Scientific Assessment of Stratospheric Ozone,* Vol. II; AFEAS Report: World Meterological Organization, Report No. 20, 1989.

(4) Thang, N. D.; Hobza, P.; Pancir, J.; Zahradnik, R. *Collect. Czech. Chem. Commun.* **1978,** *43,* 1366.

(5) (a) Williams, I. H.; Spangler, D.; Femec, D. A.; Maggiora, G. M.; Schowen, R. L. *J. Am. Chem. Soc.* **1980,** *102,* 6619. (b) Williams, I. H.; Maggiora, G. M.; Schowen, R. L. *J. Am. Chem. Soc.* **1980,** *102,* 7831. (c) Spangler, D.; Williams, I. H.; Maggiora, G. M. *J. Comput. Chem.* **1983,** *4,* 524.

(6) Williams, I. H.; Spangler, D.; Maggiora, G. M.; Schowen, R. L. *J. Am. Chem. Soc.* **1985,** *107,* 7717.

(7) Francisco, J. S.; Zhao, Y. *J. Chem. Phys.* **1992,** *96,* 7587.

(8) Yamaguchi, Y.; Goddard, J. D.; Schaefer, H. F. *J. Chem. Phys.* **1992,** *96,* 7576.

(9) Francisco, J. S. *J. Chem. Phys.* **1992,** *96,* 1167.

(10) Francisco, J. S.; Ghoul, W. *Chem. Phys.* **1991,** *257,* 89.

(11) (a) Frisch, M. J.; Head-Gordon, M.; Schlegel, H. B.; Raghavachari, K.; Binkley, J. S.; Gonzales, C.; DeFrees, D. J.; Fox, D. J.; Whiteside, R. A.; Seeger, R.; Melius, C. F.; Baker, J.; Martin, R.; Kahn, L. R.; Stewart, J. J. P.; Fluder, E. M.; Topiol, S.; Pople, J. A. *GAUSSIAN 88*; Gaussian, Inc.: Pittsburgh, PA, 1988. Frisch, M. J.; Head-Gordon, M.; Trucks, G. W.; Foresman, J. B.; Schlegel, H. B.; Raghavachari, K.; Robb, M.; Binkley, J. S.; Gonzalez, C.; DeFrees, D. J.; Fox, D. J.; Whiteside, R. A.; Seeger, R.; Melius, C. F.; Baker, J.; Martin, R. L.; Kahn, L. R.; Stewart, J. J. P.; Topiol, S.; Pople, J. A. *GAUSSIAN 90,* Revision I: Gaussian, Inc.: Pittsburgh, PA, 1990.

(12) Schlegel, H. B. *J. Comput. Chem.* **1982,** *3,* 214.

(13) Hehre, W. J.; Ditchfield, R.; Pople, J. A. *J. Chem. Phys.* **1972,** *56,* 2257.

(14) Krishnan, R.; Binkley, J. S.; Seeger, R.; Pople, J. A. *J. Chem. Phys.* **1980,** *72,* 650.

(15) Krishnan, R.; Pople, J. A. *Int. J. Quantum Chem.* **1980,** *14,* 91.

(16) Schlegel, H. B. *J. Chem. Phys.* **1986,** *84,* 4530.

(17) Pople, J. A.; Krishnan, R.; Schlegel, H. B.; Binkley, J. S. *Int. J. Quantum Chem. Symp.* **1979,** *13,* 225.

(18) Pople, J. A.; Schlegel, H. B.; Krishnan, R.; DeFrees, D. J.; Binkley, J. S.; Frisch, M. J.; Whiteside, R. A.; Hout, R. F.; Hehre, W. J. *Int. J. Quantum Chem., Quantum Chem. Symp.* **1981,** *15,* 269.

0002-7863/93/1515-3746$04.00/0

Table I. Optimized Geometries for Reactants and Products for the HXCO + H_2O Reaction[a]

		HF/6-31G*			MP2/6-31G*			MP2/6-311G**		
species	coordinate	H	F	Cl	H	F	Cl	H	F	Cl
HX	HX	0.730	0.911	1.266	0.737	0.934	1.280	0.738	0.912	1.274
H_2O	HO	0.947			0.969			0.957		
		105.5			1.040			1.025		
HXCO	CO	1.184	1.164	1.165	1.220	1.194	1.199	1.210	1.183	1.187
	CH	1.092	1.081	1.083	1.104	1.094	1.096	1.106	1.094	1.096
	CX	1.092	1.314	1.756	1.104	1.352	1.767	1.106	1.345	1.774
	HCO	122.2	126.9	126.1	122.8	127.6	126.3	122.2	127.9	126.7
	XCO	122.2	123.0	123.2	122.8	123.2	123.7	122.2	123.2	123.6
X$\ddot{C}$OH	CO	1.300	1.291	1.284	1.321	1.318	1.315	1.312	1.308	1.304
	HO	0.951	0.949	0.953	0.977	0.976	0.980	0.964	0.964	0.966
	CX	1.099	1.301	1.754	1.113	1.330	1.748	1.112	1.317	1.746
	XCO	103.1	104.8	106.6	101.5	103.9	105.6	102.0	104.7	106.2
	HOC	109.5	108.6	108.3	107.4	105.8	105.5	106.8	104.6	104.8
	XCOH	180.0	180.0	180.0	180.0	180.0	180.0	180.0	180.0	180.0
XC(O)OH	CO′	1.182	1.172	1.172	1.213	1.200	1.203	1.202	1.189	1.192
	CO	1.323	1.309	1.314	1.351	1.338	1.344	1.346	1.331	1.338
	HO	0.954	0.951	0.954	0.980	0.988	0.980	0.967	0.964	0.967
	CX	1.083	1.298	1.734	1.096	1.334	1.740	1.097	1.326	1.747
	XCO′	124.7	123.7	123.5	125.4	124.1	124.3	125.6	124.0	124.1
	OCO′	124.9	127.6	126.2	125.1	128.4	126.6	125.2	128.5	127.0
	HOC	108.7	108.7	108.0	106.1	106.3	105.6	105.6	105.6	105.2
	HOCO′	0.0	0.0	0.0	0.0	0.0	0.0	0.0	0.0	0.0
$CHX(OH)_2$	CO	1.386	1.367	1.370	1.409	1.390	1.396	1.402	1.384	1.389
	CO′	1.386	1.359	1.360	1.409	1.380	1.383	1.402	1.373	1.376
	HO	0.949	0.948	0.951	0.973	0.973	0.977	0.960	0.960	0.962
	O′H	0.949	0.951	0.951	0.973	0.976	0.977	0.960	0.963	0.964
	CH	1.083	1.079	1.076	1.094	1.093	1.091	1.094	1.091	1.089
	CX	1.083	1.341	1.792	1.094	1.368	1.787	1.094	1.361	1.788
	HOC	108.8	108.8	108.0	106.5	106.2	105.8	105.8	105.7	105.1
	HO′C	108.8	109.1	109.3	106.5	106.9	106.8	105.8	105.8	106.0
	OCO′	112.3	112.6	112.5	112.5	112.6	112.4	112.5	112.7	112.7
	XCH	109.4	108.6	106.5	109.9	108.7	107.2	109.8	108.4	106.8
	XCO′	111.8	110.8	111.5	112.3	110.3	112.2	112.2	110.8	112.2
	HO′CO	63.5	58.2	58.1	59.7	55.7	56.7	59.2	54.6	55.7
	HOCO′	60.2	58.1	59.0	59.6	57.3	57.9	59.2	56.9	56.9
	XCO′H	−55.2	−59.0	−60.9	−58.5	−60.9	−61.7	−59.1	−62.3	−63.1
	HCO′H	−174.2	−177.0	−177.1	−177.8	−179.0	−178.6	−178.3	−179.9	−179.6

[a] Bond lengths in Å and bond angles in deg.

Reaction 1. The transition structure for the addition of H_2O to HXCO (Figure 1) contains a nearly coplanar four-membered ring whose structure and energy are remarkably insensitive to the nature of the substituent X = H, F, or Cl. For the case of X = H, formation of the new CO′ σ-bond, cleavage of the CO π-bond, and transfer of H between O′ and O are coupled components of a concerted process. The imaginary frequency corresponding to the reaction coordinate vibrational mode has very similar values (2051i, 2082i, and 2057i cm^{-1}, respectively, at the HF/6-31G* level). The heat of reaction (at 0 K) is slightly exothermic for X = H (−4.8 kcal mol^{-1}), but slightly endothermic for X = F and Cl (2.4 and 3.2 kcal mol^{-1}, respectively). Correspondingly, the barrier heights increase slightly from 40.9 to 43.1 and then 43.6 kcal mol^{-1} along this series, and simple Hammond-postulate considerations would suggest that the position of the transition state along the reaction coordinate might become more advanced. The CO′ bond length in the transition structure does indeed decrease from 1.678 Å (X = H) to 1.631 Å (X = F) and then 1.609 Å (X = Cl) in accord with this simple expectation, but a fuller analysis of the relationship between energetic variations and transition-state structural changes would require a multidimensional treatment of the reaction coordinate.

The effect of electron correlation at the MP2 level diminishes the barrier height markedly, by 14 or 15 kcal mol^{-1} with the 6-31G* basis set for each substituent X, but alters the reaction energy by a much smaller amount. Use of the full MP4 method with a substantially larger 6-311++G** basis raises the barrier height and decreases the reaction exothermicity by 3 or 4 kcal mol^{-1} in each case.

Reaction 2. The lowest energy path for unimolecular decomposition of $CHX(OH)_2$, where X = F or Cl, is 1,2-elimination of HX, yielding formic acid HC(O)OH via the four-center transition structure shown in Figure 1b. This structure is very sensitive not only to the nature of X but also to the basis set and theoretical method employed. In each structure the CX bond is largely broken, the HX bond is only slightly formed, and the leaving group X bears a partial negative charge. With X = F, the transition state is tighter, with Pauling bond orders of 0.22 and 0.33 respectively for the CF and HF bonds, and a reaction-coordinate vibrational frequency of 1608i cm^{-1}. With X = Cl, the transition state is looser, with Pauling bond orders of 0.09 and 0.10 respectively for the CCl and HCl bonds, and a reaction-coordinate vibrational frequency of only 174i cm^{-1}. However, the OH bond to the leaving hydrogen is more broken in the transition state for X = F than for X = Cl (Pauling bond order 0.49 versus 0.83). The 1,2-elimination, while being concerted, tends to proceed asynchronously with inital departure of X^- from carbon being followed by abstraction of H^+ from oxygen; this tendency is greater for the better leaving group X = Cl.

1,2-Elimination of HX is slightly more exothermic for X = F than for X = Cl (−14.8 versus −12.3 kcal mol^{-1}) but has a slightly higher barrier (28.6 versus 26.6 kcal mol^{-1}) at the MP4 level. Hammond-postulate considerations do not apply in this case. Inclusion of electron correlation at the MP2 level substantially reduces the barrier for X = F, but raises it for X = Cl. The barrier for HF elimination is only about a half of that calculated for the analogous elimination from CF_3OH yielding CF_2O.[19]

Reaction 3. Besides elimination of H_2O (the reverse of reaction 1) and elimination of HX, a third mode of decomposition for the $CHX(OH)_2$ adducts is 1,2-elimination of H_2 via another four-

---

(19) Francisco, J. S. *Chem. Phys.* **1991**, *150*, 19.

Table II. Optimized Geometries for Transition States for $HXCO + H_2O \rightarrow CXH(OH)_2 \rightarrow$ Products

		HF/6-31G*			MP2/6-31G*			MP2/6-311G**		
reaction	coordinate	H	F	Cl	H	F	Cl	H	F	Cl
$HXCO + H_2O \rightarrow CXH(OH)_2$	CO	1.294	1.269	1.270	1.309	1.281	1.282	1.300	1.272	1.272
	CO′	1.639	1.582	1.557	1.676	1.624	1.607	1.678	1.631	1.609
	OH	1.324	1.326	1.343	1.356	1.345	1.354	1.330	1.316	1.330
	O′H	0.953	0.955	0.956	0.981	0.982	0.984	0.967	0.969	0.970
	CH	1.083	1.077	1.076	1.098	1.092	1.092	1.098	1.091	1.090
	CX	1.088	1.339	1.817	1.403	1.383	1.840	1.103	1.372	1.837
	OCO′	93.3	94.8	95.5	94.4	95.5	96.0	94.1	95.1	95.8
	HOC	77.2	77.4	77.0	76.9	77.5	77.3	75.8	76.6	76.3
	H′O′C	113.9	112.7	114.5	108.4	107.2	109.1	107.9	107.9	108.8
	HCO	119.6	122.0	122.2	119.9	122.7	122.9	120.0	123.3	123.3
	XCO	119.5	117.8	118.0	119.7	118.0	118.4	119.5	117.9	118.3
	HCX	112.4	108.8	106.3	112.1	107.9	105.8	112.6	107.9	106.0
	HO′CO	0.02	3.8	3.1	–1.4	5.7	4.6	–1.0	4.7	4.2
	HCO′H	105.8	116.1	116.2	103.5	119.1	118.0	103.7	116.9	116.9
	XCO′H	–108.6	–104.6	–108.3	–110.6	–101.8	–105.9	–109.5	–103.4	–106.4
$CXH(OH)_2 \rightarrow XC(O)OH + H_2$	CO	1.274	1.278	1.282	1.322	1.297	1.299	1.310	1.286	1.287
	CO′	1.277	1.305	1.316	1.341	1.339	1.348	1.334	1.333	1.340
	CH	2.016	1.502	1.439	1.502	1.440	1.414	1.516	1.452	1.433
	OH	1.080	1.266	1.309	1.319	1.335	1.362	1.304	1.316	1.343
	HH	1.318	1.023	0.983	1.025	1.009	0.990	1.013	1.000	0.986
	O′H	0.956	0.952	0.954	0.980	0.977	0.980	0.967	0.964	0.967
	CX	1.067	1.298	1.758	1.094	1.346	1.787	1.094	1.337	1.786
	HCO	80.3	96.4	99.3	99.2	102.0	103.8	98.1	100.8	102.5
	HOC	89.9	68.0	64.7	63.4	62.6	60.8	64.1	63.2	61.6
	HO′C	110.2	108.5	107.3	105.1	105.6	104.6	104.7	104.9	104.1
	XCO	124.2	119.6	119.8	122.0	119.7	119.9	122.4	119.8	119.9
	OCO	120.0	121.4	119.7	119.1	120.8	119.7	119.7	121.6	120.6
	XCO′	114.1	110.2	110.2	109.7	108.3	108.2	109.4	108.2	108.2
	HCOH	–8.3	–1.9	–1.0	–5.0	–2.6	–2.1	–4.6	–2.7	–2.6
	HO′CO	14.0	15.3	12.6	18.4	15.0	14.2	18.9	16.2	15.7
$CXH(OH)_2 \rightarrow X\ddot{C}OH + H_2O$	CO	1.963	1.941	1.914	2.055	1.966	1.993	2.012	1.937	1.961
	CO′	1.300	1.283	1.289	1.320	1.308	1.311	1.317	1.303	1.307
	CH′	1.222	1.188	1.206	1.287	1.218	1.241	1.260	1.205	1.223
	H′O	1.244	1.298	1.264	1.188	1.275	1.243	1.192	1.271	1.243
	CX	1.081	1.303	1.739	1.099	1.346	1.752	1.097	1.337	1.751
	OH	0.951	0.952	0.952	0.978	0.980	0.980	0.965	0.967	0.967
	O′H	0.951	0.956	0.954	0.978	0.983	0.983	0.965	0.970	0.969
	H′CO	37.6	40.7	40.3	32.3	40.0	36.7	33.8	40.0	37.7
	XCO	98.4	102.7	104.5	96.4	100.6	103.3	96.3	101.1	103.5
	HOH	107.2	102.3	100.1	108.4	101.6	99.4	108.3	102.3	100.1
	O′CO	108.2	107.9	105.8	107.4	106.5	105.0	107.1	106.1	104.7
	HOC	107.2	109.6	110.5	102.4	100.9	102.7	100.1	99.7	101.1
	HO′C	113.5	112.0	114.0	112.6	109.8	112.6	110.9	108.7	110.7
	XCO′	114.5	112.2	114.7	112.6	111.4	114.1	113.0	111.7	114.3
	HOH′C	98.9	98.3	100.1	93.6	92.7	94.8	93.4	93.7	95.1
	XCOH′	125.1	130.1	129.4	119.4	121.6	120.9	118.6	120.9	118.5
$CXH(OH)_2 \rightarrow HC(O)OX + HX$	CO		1.275	1.258		1.299	1.281		1.293	1.277
	CO′		1.284	1.268		1.318	1.298		1.308	1.293
	CX		1.888	2.682		1.819	2.592		1.832	2.522
	OH		1.106	0.972		1.176	1.020		1.133	1.018
	HX		1.273	2.345		1.244	2.093		1.260	1.965
	O′H		0.955	0.953		0.981	0.978		0.968	0.966
	CH		1.071	1.068		1.087	1.018		1.086	1.082
	XCO		83.4	87.2		86.5	84.8		86.0	84.2
	HOC		87.6	107.5		83.8	101.8		83.8	98.7
	HCO		123.1	122.2		123.6	122.9		123.4	122.7
	OCO		120.6	116.4		119.8	115.5		120.1	116.2
	HO′C		109.9	112.7		106.5	110.4		106.0	109.2
	HOCX		–3.0	23.6		–3.1	19.6		–3.6	16.4
	HO′CO		14.3	179.0		16.1	175.0		15.9	174.4
	XCH		92.8	63.4		94.9	68.2		94.0	74.7
	XCO′		110.9	127.8		111.8	129.4		111.8	125.5

[a] Bond lengths in Å and bond angles in deg.

center transition structure, as shown in Figure 1c. Both the CH and OH bonds are substantially broken in this structure (Pauling bond orders in the range 0.24 to 0.32), but the balance between them varies somewhat with the nature of the substituent X. In the transition state for X = H, the CH bond is weaker and the OH bond stronger, whereas with X = Cl it is the other way around, and also the HH bond is slightly stronger (Pauling bond order of 0.44 versus 0.40). This small degree of structural variation with X is reflected in the barrier heights, which diminish from 83.2 to 80.9 and then to 77.6 kcal mol^{-1} as the substituent is changed from H to F and then to Cl, but this systematic trend is not found in the heats of reaction (which are close to thermoneutral for each substituent). These barrier heights are, of course, very much greater than those for HX elimination or for the reverse of reaction 1, but are comparable with those calculated for 1,2-elimination of H_2 from ethylsilane (107 kcal mol^{-1}, leading to $SiH_2{=}CHCH_3$)[20] and ethane (122 kcal mol^{-1}, leading to ethene).[21]

Reaction 4. A 1,2-hydrogen shift may occur from carbon to oxygen accompanied by cleavage of the same CO bond to yield

Table III. Total Energies (Hartrees) for Species Involved in the HXCO + H_2O Reaction

species	HF/6-31G*	MP2/6-31G*	MP2/6-311G**	MP4SDTQ/6-311++G**//MP2/6-311G**
		Reactants and Products		
H_2	−1.126 83	−1.144 14	−1.160 27	−1.167 76
HF	−100.002 91	−100.184 16	−100.286 08	−100.286 21
HCl	−460.059 98	−460.20 25	−460.292 97	−460.263 84
CO	−112.737 88	−113.028 18	−113.111 42	−113.102 13
H_2O	−76.010 75	−76.199 24	−76.282 89	−76.287 21
H_2CO	−113.866 33	−114.174 96	−114.272 43	−114.269 40
HFCO	−212.747 84	−213.229 26	−213.397 53	−213.381 19
HClCO	−572.781 61	−573.233 46	−573.394 99	−573.356 56
HCOH	−113.783 52	−114.077 05	−114.183 66	−114.184 88
FCOH	−212.678 32	−213.146 97	−213.321 86	−213.310 92
ClCOH	−572.706 99	−573.144 44	−573.312 40	−573.279 56
HC(O)OH	−188.762 31	−189.251 87	−189.408 04	−189.394 77
FC(O)OH	−287.632 80	−288.290 03	−288.514 58	−288.489 65
ClC(O)OH	−647.663 46	−648.295 23	−648.514 58	−648.467 00
$CH_2(OH)_2$	−189.900 63	−190.397 61	−190.578 04	−190.574 41
$CHF(OH)_2$	−288.773 00	−289.438 97	−289.689 72	−289.672 26
$CHCl(OH)_2$	−648.805 33	−649.442 95	−649.686 95	−649.646 96
		Transition States		
$H_2CO + H_2O \rightarrow CH_2(OH)_2$	−189.798 42	−190.318 00	−190.497 64	−190.494 38
$CH_2(OH)_2 \rightarrow HC(O)OH + H_2$	−189.740 98	−190.255 84	−190.443 78	−190.440 53
$CH_2(OH)_2 \rightarrow HCOH + H_2O$	−189.742 41	−190.259 93	−190.447 39	−190.449 44
$HCO \rightarrow H_2CO$	−113.699 63	−114.026 26	−114.132 53	−114.132 60
$HCOH \rightarrow H_2 + CO$	−113.655 88	−113.977 27	−114.093 49	−114.095 40
$HFCO + H_2O \rightarrow CHF(OH)_2$	−288.678 04	−289.370 42	−289.619 69	−289.601 68
$CHF(OH)_2 \rightarrow HC(O)OH + HF$	−288.699 83	−289.384 26	−289.635 16	−289.621 03
$CHF(OH)_2 \rightarrow FC(O)OH + H_2$	−288.610 41	−289.299 57	−289.558 11	−289.540 52
$CHF(OH)_2 \rightarrow FCOH + H_2O$	−288.616 59	−289.309 50	−289.564 42	−289.552 75
$FCOH \rightarrow HFCO$	−212.587 51	−213.092 12	−213.267 57	−213.255 27
$FCOH \rightarrow HF + CO$	−212.617 04	−213.108 65	−213.280 67	−213.270 96
$HClCO + H_2O \rightarrow CHCl(OH)_2$	−648.709 34	−649.373 78	−649.616 66	−649.576 39
$CHCl(OH)_2 \rightarrow HC(O)OH + HCl$	−648.773 98	−649.400 54	−649.647 44	−649.603 72
$CHCl(OH)_2 \rightarrow ClC(O)OH + H_2$	−648.635 84	−649.298 80	−649.550 85	−649.512 68
$CHCl(OH)_2 \rightarrow ClCOH + H_2O$	−648.648 69	−649.313 82	−649.562 50	−649.529 91
$ClCOH \rightarrow HClCO$	−572.623 03	−573.096 14	−573.263 50	−573.229 14
$ClCOH \rightarrow HCl + CO$	−572.670 96	−573.110 01	−573.283 98	−573.249 05

H_2O and a carbene XCOH. This is a concerted process, occurring by means of the transition structure shown in Figure 1d. The barriers for this reaction are about 10 kcal mol^{-1} lower than for reaction 3, and follow the same trend along the series X = H, F, and Cl; nonetheless, the respective barrier heights of 73.1, 70.1, and 68.4 kcal mol^{-1} are still much higher than those for reactions 2 or −1.

Reaction 5. The carbenes XCOH may undergo intramolecular rearrangement to the carbonyl compounds HXCO, as discussed elsewhere.[7] These rearrangements are very exothermic, and their barrier heights are relatively insensitive to the nature of X (28.4 31.2, and 27.7 kcal mol^{-1} respectively for X = H, F, and Cl).

Reaction 6. Dissociation of the carbenes XCOH to HX + CO is 8–12 kcal mol^{-1} more exothermic than intramolecular rearrangement. For X = H the barrier height for dissociation is, at 48.6 kcal mol^{-1}, considerably higher than for rearrangement, but for X = F and Cl the dissociation barriers (21.0 and 15.3 kcal mol^{-1}, respectively) are significantly lower than for reaction 5. These processes have been discussed in detail previously.[7]

Overview of Homogeneous HXCO Hydrolysis. Addition of H_2O to H_2CO yields the hydrate $CH_2(OH)_2$ which is then stable to further decomposition (except the reverse of its formation by reaction 1); the barriers to elimination of H_2 or H_2O by means of either reaction 3 or reaction 4 are too high to be of significance.

The adduct $CHF(OH)_2$ may easily undergo 1,2-elimination of HF (reaction 2) to yield formic acid HC(O)OH as a product. Once the initial 43.1 kcal mol^{-1} barrier for addition of H_2O to HFCO has been surmounted, there should be sufficient chemical activation to overcome the 28.6 kcal mol^{-1} barrier for decomposition by this route. Similarly, the 43.6 kcal mol^{-1} barrier for addition of H_2O to HClCO should mean that the adduct $CHCl(OH)_2$ possesses sufficient energy to overcome the 26.6 kcal mol^{-1} barrier for 1,2-elimination of HCl to yield formic acid also.

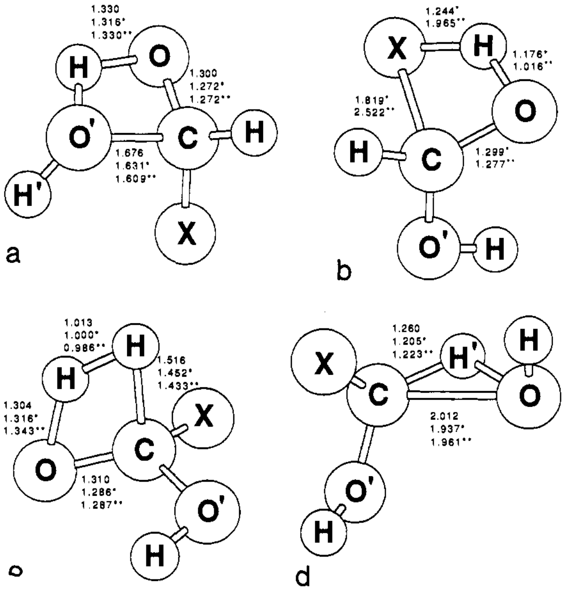

Figure 1. MP2/6-311G** optimized transition structures: no asterisk, X = H; single asterisk (*), X = F; double asterisk (**), X = Cl. (a) Reaction 1: $H_2O + HXCO \rightarrow CHX(OH)_2$. (b) Reaction 2: $CHX(OH)_2 \rightarrow HC(O)OH + HX$. (c) Reaction 3: $CHX(OH)_2 \rightarrow XC(O)OH + H_2$. (d) Reaction 4: $CHX(OH)_2 \rightarrow XCOH + H_2O$.

---

(20) Francisco, J. S. *J. Chem. Phys.* **1988**, *88*, 3767.

(21) Gordon, M. S.; Truong, T. N.; Pople, J. A. *Chem. Phys. Lett.* **1986**, *130*, 245.

Table IV. Vibration Frequencies (cm^{-1}) and Zero-Point Energies (kcal mol^{-1}) for Species Involved in the HXCO + H_2O Reaction

species	frequencies (HF/6-31G*)	ZPE
	Reactants and Products	
H_2	4643	6.6
HF	4357	6.3
HCl	3183	4.6
CO	2439	3.5
H_2O	4189, 4071, 1827	14.4
H_2CO	3232, 3160, 2028, 1680, 1383, 1335	18.3
HFCO	3360, 2103, 1539, 1248, 1173, 738	14.5
HClCO	3316, 2043, 1492, 1070, 827, 511	13.2
HCOH	4048, 3100, 1646, 1447, 1332, 1127	18.2
FCOH	4101, 1534, 1414, 1197, 786, 714	13.9
ClCOH	4035, 1478, 1418, 784, 761, 496	12.8
HC(O)H	4038, 3322, 2035, 1552, 1441, 1275, 1192, 718, 692	23.2
FC(O)OH	4081, 2107, 1566, 1360, 1081 886, 680, 622, 611	18.6
ClC(O)OH	4032, 2959, 1474, 1306, 803, 790 594, 546, 449	17.2
$CH_2(OH)_2$	4093, 1092, 3293, 3245, 1697, 1610, 1528 1506, 1319, 1232, 1166, 1102, 618, 438, 410	39.1
$CHF(OH)_2$	4108, 4063, 3329, 1621, 1583, 1449, 1402 1302, 1233, 1109, 717, 610, 555, 414, 303	34.0
$CHCl(OH)_2$	4068, 4064, 3353, 1584, 1532, 1412, 1357 1283, 1177, 781, 658, 522, 419, 390, 313	32.8
	Transition States	
$H_2CO + H_2O \rightarrow CH_2(OH)_2$	4058, 3295, 3211, 2206, 1737, 1501, 1487 1412, 1321, 1184, 908, 822, 575, 495, 2051i	34.6
$CH_2(OH)_2 \rightarrow HC(O)OH + H_2$	4008, 3517, 2285, 1731, 1564, 1515, 1397 1299, 1197, 1127, 885, 739, 643, 155, 2188i	31.5
$CH_2(OH)_2 \rightarrow HCOH + H_2O$	4066, 4036, 3308, 2378, 1659, 1563, 1411 1325, 1143, 831, 679, 530, 450, 251, 1914i	33.8
$HCOH \rightarrow H_2CO$	3167, 2819, 1652, 1432, 649, 2710i	13.9
$HCOH \rightarrow H_2 + CO$	2282, 1795, 1698, 1019, 694, 3242i	10.7
$HFCO + H_2O \rightarrow CHF(OH)_2$	4035, 3369, 2260, 1655, 1495, 1457, 1358 1270, 996, 901, 721, 630, 535, 384, 2082i	30.1
$CHF(OH)_2 \rightarrow HC(O)OH + HF$	4017, 3467, 2326, 1734, 1523, 1478, 1311 1253, 1053, 872, 699, 639, 543, 232, 1608i	30.2
$CHF(OH)_2 \rightarrow HC(O)OH + H_2$	4071, 2149, 1899, 1687, 1587, 1327, 1275 1152, 890, 732, 678, 602, 569, 404, 2735i	27.2
$CHF(OH)_2 \rightarrow FCOH + H_2O$	4062, 3989, 2534, 1602, 1496, 1458, 1199 832, 800, 664, 585, 494, 277, 245, 1923i	28.9
$FCOH \rightarrow HFCO$	2787, 1810, 1267, 718, 306, 2499i	9.8
$FCOH \rightarrow HF + CO$	2302, 1876, 162, 898, 676, 1924i	9.9
$HClCO + H_2O \rightarrow CHCl(OH)_2$	4021, 3366, 2282, 1553, 1464, 1448, 1332 1142, 896, 758, 683, 497, 422, 328, 2057i	28.9
$CHCl(OH)_2 \rightarrow HC(O)OH + HCl$	4051, 3726, 3499, 1826, 1601, 1497, 1350, 1287, 1027, 739, 673, 631, 446, 234, 174i	32.3
$CHCl(OH)_2 \rightarrow ClC(O)OH + H_2$	4032, 2173, 1980, 1605, 1491, 1306, 1252 890, 767, 762, 672, 504, 435, 384, 2729i	26.1
$CHCl(OH)_2 \rightarrow ClCOH + H_2O$	4070, 3996, 2450, 1567, 1464, 1399, 896 799, 701, 594, 500, 481, 269, 229, 1978i	27.8
$ClCOH \rightarrow HClCO$	1784, 1723, 777, 489, 420, 2537i	8.9
$ClCOH \rightarrow HCl + CO$	2407, 1847, 902, 810, 363, 1002i	9.0

Reactions 3, 4, 5, and 6 are of no importance for the hydrolysis mechanisms of HFCO and HClCO in view of the much higher barriers involved.

Libuda et al.[22] recently measured the room-temperature rate coefficient for the reaction of H_2O with HClCO; this reaction was found to be faster than that of H_2O with Cl_2CO studied by Butler and Snelson.[23] Since the reported[23] activation energy for the latter reactions is 14 kcal mol^{-1}, it would be reasonable to expect the activation energy for H_2O + HClCO to have a smaller value. The present calculations predict a potential energy barrier height of ~44 kcal mol^{-1}, which cannot be reconciled with such a low activation energy.

It is worth pointing out that for addition of H_2O to H_2CO it has been predicted that a second molecule of water may catalyze the reaction very effectively by participating in a cyclic transition structure.[24] The presence of the extra water molecule reduces the ideal-gas-phase HF/STO-3G calculated free energy of activation for the hydration from 53.4 to 26.5 kcal mol^{-1} (25 °C, 1 atm), despite this reaction being an entropically disfavored termolecular process. This dramatic catalytic effect has been confirmed by recent calculations[25] at the BAC-MP4/6-31G** level; the barrier for reaction from the hydrogen-bonded encounter complex is reduced from 41.0 to 20.3 kcal mol^{-1} (cf. 45.6 to 10.1 kcal mol^{-1} at the HF/STO-3G level[24]). It is therefore reasonable to expect that addition of H_2O to HFCO or to HClCO may also be subject to catalysis in the same manner, and to suppose that this may account for the rather low activation energy implied by the experimental results of Libuda et al.[22] Thus the present calculated results may not be directly comparable with the experimental data mentioned above.[22,23] Furthermore, it is entirely conceivable that decomposition of the adducts by 1,2-

---

[22] Libuda, H. G.; Zabel, F.; Fink, E. H.; Becker, K. H. *J. Phys. Chem.* **1990**, *94*, 5860.

[23] Butler, R. Snelson, A. J. *Air Pollut. Control Assoc.* **1979**, *29*, 833.

[24] Williams, I. H.; Spangler, D.; Femec, D. A.; Maggiora, E. M.; Schowen, R. L. *J. Am. Chem. Soc.* **1983**, *105*, 31.

[25] Garrett, B. C.; Melius, C. F. In *Theoretical and Computational Models for Organic Chemistry* (NATO ASI); Kluwer: Dordrecht, 1991.

Table V Heats of Reactions and Barrier Heights (kcal mol^{-1}) for HXCO + H_2O Reaction

reaction process	HF/6-31G*	MP2/6-31G*	MP2/6-311G**	MP4/6-311++G**// MP2/6-311G**	ΔZPE	MP4/6-311++G**// MP2/6-311G** + ΔZPE
$H_2CO + H_2O \rightarrow CH_2(OH)_2$	−14.8	−14.7	−14.3	−11.2	6.4	−4.8
$[H_2CO + H_2O \rightarrow CH_2(OH)_2]^{\ddagger}$	49.3	35.3	36.1	39.0	1.9	40.9
$CH_2(OH)_2 \rightarrow HC(O)OH + H_2$	7.2	1.0	1.9	7.4	−9.3	−1.9
$[CH_2(OH)_2 \rightarrow HC(O)OH + H_2]^{\ddagger}$	100.2	89.0	84.2	84.0	−0.8	83.2
$CH_2(OH)_2 \rightarrow HCOH + H_2O$	66.7	76.1	70.0	64.2	−6.5	57.7
$[CH_2(OH)_2 \rightarrow HCOH + H_2O]^{\ddagger}$	99.3	86.4	82.0	78.4	−5.3	73.1
$HCOH \rightarrow H_2CO$	−52.0	−61.4	−55.7	−53.0	0.1	−52.9
$[HCOH \rightarrow H_2CO]^{\ddagger}$	52.6	31.9	32.1	32.8	−4.4	28.4
$HCOH \rightarrow H_2 + CO$	−50.9	−59.8	−55.2	−53.3	−8.1	−61.4
$[HCOH \rightarrow H_2 + CO]^{\ddagger}$	80.1	62.6	56.6	56.1	−7.5	48.6
$HFCO + H_2O \rightarrow CHF(OH)_2$	−9.0	−6.6	−5.8	−2.7	5.1	2.4
$[HFCO + H_2O \rightarrow CHF(OH)_2]^{\ddagger}$	50.5	36.4	38.1	41.9	1.2	43.1
$CHF(OH)_2 \rightarrow HC(O)OH + HF$	4.7	1.8	−2.8	−5.2	−9.6	−14.8
$[CHF(OH)_2 \rightarrow HC(O)OH + HF]^{\ddagger}$	45.9	34.3	34.2	32.4	−3.8	28.6
$CHF(OH)_2 \rightarrow FC(O)OH + H_2$	8.4	3.0	7.5	9.6	−8.8	0.8
$[CHF(OH)_2 \rightarrow FC(O)OH + H_2]^{\ddagger}$	102.0	87.5	82.6	82.9	−2.0	80.9
$CHF(OH)_2 \rightarrow FCOH + H_2O$	52.7	58.2	53.3	46.8	−5.7	41.1
$[CHF(OH)_2 \rightarrow FCOH + H_2O]^{\ddagger}$	98.1	81.2	78.6	75.2	−5.1	70.1
$FCOH \rightarrow HFCO$	−43.6	−51.6	−45.9	−44.1	0.6	−43.5
$[FCOH \rightarrow HFCO]^{\ddagger}$	57.0	34.4	34.1	34.9	−3.7	31.2
$FCOH \rightarrow HF + CO$	−39.2	−41.0	−47.5	−48.6	−4.1	−52.7
$[FCOH \rightarrow HF + CO]^{\ddagger}$	38.4	24.0	25.8	25.0	−4.0	21.0
$HClCO + H_2O \rightarrow CHCl(OH)_2$	−8.1	−6.4	−5.7	−2.0	5.2	3.2
$[HClCO + H_2O \rightarrow CHCl(OH)_2]^{\ddagger}$	52.1	37.0	38.4	42.3	1.3	43.6
$CHCl(OH)_2 \rightarrow HC(O)OH + HCl$	−10.6	−6.9	−8.8	−7.3	−5.0	−12.3
$[CHCl(OH)_2 \rightarrow HC(O)OH + HCl]^{\ddagger}$	19.7	26.6	24.8	27.1	−0.5	26.6
$CHCl(OH)_2 \rightarrow ClC(O)OH + H_2$	9.4	2.2	7.6	7.7	−9.0	−1.3
$[CHCl(OH)_2 \rightarrow ClC(O)OH + H_2]^{\ddagger}$	106.4	90.4	85.4	84.3	−6.7	77.6
$CHCl(OH)_2 \rightarrow ClCOH + H_2O$	55.0	62.3	57.5	50.3	−5.6	44.7
$[CHCl(OH)_2 \rightarrow ClCOH + H_2O]^{\ddagger}$	98.3	81.0	78.1	73.4	−5.0	68.4
$ClCOH \rightarrow HClCO$	−46.8	−55.9	−51.8	−48.3	1.7	−46.6
$[ClCOH \rightarrow HClCO]^{\ddagger}$	52.7	30.3	30.7	31.6	−3.9	27.7
$ClCOH \rightarrow HCl + CO$	−57.0	−53.9	−57.7	−54.2	−4.7	−58.9
$[ClCOH \rightarrow HCl + CO]^{\ddagger}$	24.4	21.6	17.8	19.9	−3.8	15.3

elimination of HX may also be subject to catalysis; since similar reductions in barrier heights would be expected as for hydration, it is not anticipated that the involvement of catalysis by water would qualitatively alter the relative energetics of the alternative decomposition pathways for the $CHX(OH)_2$ adducts.

Acknowledgment. I.H.W. thanks the SERC and the Royal Society for financial support. J.S.F. is grateful to the National Science Foundation for the award of a Presidential Young Investigation Award and to the A.P. Sloan Foundation for a Research Fellowship.